Journal of Luminescence 177 (2016) 139–144

Contents lists available at ScienceDirect

Journal of Luminescence

journal homepage: www.elsevier.com/locate/jlumin

Full Length Article

Centers responsible for the TL peaks of willemite mineral estimated by EPR analysis

T.K. Gundu Rao [a], Nilo F. Cano [b,*], Betzabel N. Silva-Carrera [a], Reinaldo M. Ferreira [a], Henry S. Javier-Ccallata [c,*], Shigueo Watanabe [a,*]

[a] Instituto de Física, Universidade de São Paulo, Rua do Matão, Travessa R, 187, CEP 05508-090, São Paulo, SP, Brazil
[b] Departamento de Ciências do Mar, Universidade Federal de São Paulo, Rua Doutor Carvalho de Mendonça, 144, CEP 11070-102, Santos, SP, Brazil
[c] Escuela Profesional de Física, Facultad de Ciencias Naturales y Formales, Universidad Nacional de San Agustín (UNSA), Av. Independencia S/N, Arequipa, Peru

ARTICLE INFO

Article history:
Received 6 January 2016
Received in revised form
17 March 2016
Accepted 13 April 2016
Available online 23 April 2016

Keywords:
TL
EPR
Silicates
Willemite

ABSTRACT

The mineral willemite (Zn_2SiO_4) exhibits five thermoluminescence (TL) peaks approximately at 160, 225, 260, 310 and 400 °C. Electron paramagnetic resonance (EPR) studies were carried out to study the defect centers induced in the mineral by gamma irradiation and also to identify the centers responsible for the TL process. Room temperature EPR spectrum of irradiated mineral is a superposition of at least four distinct centers. One of the centers (center I) with an isotropic g factor 2.0114 is attributable to an intrinsic O^- type center and the center correlates with the TL peak at 160 °C. Center II exhibiting hyperfine lines is also tentatively assigned to an O^- ion and is related to the low temperature TL peak at 160 °C. Center III is characterized by an axially symmetric g-tensor with principal values $g_{\parallel}=2.0451$ and $g_{\perp}=2.011$ and is identified as an O_2^- ion. This center appears to be related to 160, 225 and 260 °C TL peaks. Center IV with principal g-values $g_{\parallel}=2.0025$ and $g_{\perp}=2.0088$ is attributed to an F^+-type center (singly ionized oxygen vacancy) and is the likely recombination center for TL peaks between 160 and 310 °C.

1. Introduction

Silicate minerals are found abundantly in the Earth crust. They are ionic crystals in which anions can be tetrahedral SiO_4 or complex molecules formed by coupling of SiO_4 tetrahedra. One, two, up to five valence cations can be bonded to produce a very large variety of crystals of silicate. The natural minerals of silicate during their formation have incorporated large number of impurities that influence profoundly the proprieties of minerals. These impurities together with thermodynamically produced point defects are, of course, basic of mineral physical proprieties and how to correlate them is an important and not easy task to be carried out.

Willemite, Zn_2SiO_4, is isomorphous with phenakite (Be_2SiO_4) and phenakite belongs to $C_{3h}^2(R\,3)$ point group. The rhombohedral unit cell has parameters 0.768 nm and 108° 1′ and the hexagonal $a=1.242$ nm and $c=0.821$ nm [1]. Willemite is a silicate of individual unlinked silicon tetrahedra. Each zinc is also at the center of the oxygen tetrahedral of almost the same size as the silicon tetrahedron. These tetrahedral are linked together in a chain running parallel to the hexagonal c axis. Each oxygen has two zinc and one silicon atoms at the corners of an equilateral triangle.

In a perfect lattice, Si and Zn atoms are expected to be located in their respective sites. However, antisite cation exchange is likely to exist in Zn_2SiO_4 wherein Si atoms will partially replace Zn sites. These replacements, called as cation exchange disorder, are a point defect in crystal lattices. The occurrence of such defects has been predicted by theoretical calculations [2]. X-ray diffraction [3] and X-ray absorption fine structure [4] investigations support this prediction. In recent years, it has also been possible to directly observe these defects by advanced electron microscopy [5]. This mineral has been investigated experimentally by many authors due to its luminescence properties. Luminescence properties may be affected by these defects and a recent study of Cr^{3+} doped AB_2O_4 spinels has demonstrated the effects of such defects [6]. The luminescence of the synthetic willemite doped with Eu^{3+}, Mn^{2+}(Tb^{3+}), or Ce^{3+} covers the red, green, and blue portions of the visible spectrum, respectively [7–10]. A process of irradiation and thermal treatment can change the luminescent properties of the crystals [11–13]. Due to their high luminescence, the sample natural willemite can be used in the dosimetry by TL and EPR.

As far as we know, no work has been published on TL and EPR of willemite crystal up to the present. The objective of the present work is to study the nature of the luminescence and paramagnetic

* Corresponding authors.
E-mail addresses: nilo.cano@unifesp.br, nilocano@if.usp.br (N.F. Cano), henrysjc@gmail.com (H.S. Javier-Ccallata), watanabe@if.usp.br (S. Watanabe).

http://dx.doi.org/10.1016/j.jlumin.2016.04.026
0022-2313/

centers in natural willemite, measuring the effects of gamma irradiation and thermal treatments through electron paramagnetic resonance (EPR) technique in an attempt to understand some physical properties and seeking possible applications in the area of ionizing radiation dosimetry of this mineral.

2. Materials and methods

Willemite of chemical formula Zn_2SiO_4 here investigated is a natural silicate mineral from Mexico, purchased through stone dealer Luis Menezes Minerals Ltd. in Belo Horizonte, MG. This mineral together with olivine, phenakite and zircon belongs to the group of olivine.

The TL measurements were carried out in a nitrogen atmosphere with a model 4500 Harshaw TL reader equipped with two photomultiplier tubes, which could record luminescence independently. The reader was controlled by WinRems software supplied with the spectrometer and running on a Windows computer. The heating rate used in the TL measurements was 5 °C/s. Each point in the glow curve represents an average of five reading.

EPR experiments were carried out using a Bruker EMX EPR spectrometer operating at X-band frequency with 100 kHz modulation frequency. The *g*-factor of signals were determined using a reference sample of Diphenyl Picryl Hydrazyl (DPPH). Temperature dependence of the EPR spectra was studied using a Bruker BVT 2000 variable temperature accessory.

For TL and EPR measurements a fraction of crystals have been crushed and sieved retaining grains of size 0.080 and 0.180 mm diameters. Grains smaller than 0.080 mm were used in the X-ray fluorescence (XRF) and X-ray diffraction analysis. The X-ray fluorescence (XRF) technique was used to find the elemental composition of the mineral and the X-ray diffraction technique was utilized for the structural analysis.

For irradiation, IPEN/CNEN/SP – Institute for Energy and Nuclear Researches Radiation Center's ^{60}Co source was used.

3. Results and discussion

The diffractograms of the willemite crystal is shown in Fig. 1, together with that of a standard willemite crystal. Comparing the powder XRD pattern to the JCPDS files, all the peaks of the crystal are identified as belonging to willemite (JCPDS card, No. 37-1485), as shown in Fig. 1. An analysis of the main oxide components of the willemite crystal was obtained by X-ray fluorescence (XRF). Results are presented in Table 1. This analysis was performed to identify the chemical elements in the sample, and for future studies about which of these elements are responsible for the TL signal. Besides SiO_2 and ZnO that are basic components, Al_2O_3, Fe_2O_3 and CaO appear as impurities in small but considerable amount. The role of these impurities is something to be investigated. From the comparison of experimental results with the XRD pattern of the willemite, it was inferred that other parasitic phases are not present in the sample. Therefore, it may be concluded that impurities such as Al_2O_3, Fe_2O_3 and CaO are diluted in the crystal of willemite as impurities.

In natural willemite mineral, TL glow peaks are not observed. TL glow curves of willemite samples heat-treated at 500 °C for 30 min and irradiated with γ-doses from 10 Gy to 2.5 kGy show four TL peaks at 160, 225 and 310 °C whilst a smaller broad peak is seen around 390 °C. The TL glow curves are shown in Fig. 2. The inset of Fig. 2 shows the behavior of TL peaks with γ-dose. All TL peaks grow linearly up to about 200 Gy and supra-linearly between 200 Gy and 2 kGy and then the three main TL peaks saturate.

The TL glow curve of the willemite crystal was analyzed by the E–T_{stop} [14, 15] and CGCD [16] methods and the characteristic parameters (i.e. E, s, and the lifetime) for each peak were calculated.

Fig. 3 shows the obtained activation energies (E) using the E–T_{stop} method. With these results and applying the CGCD equations

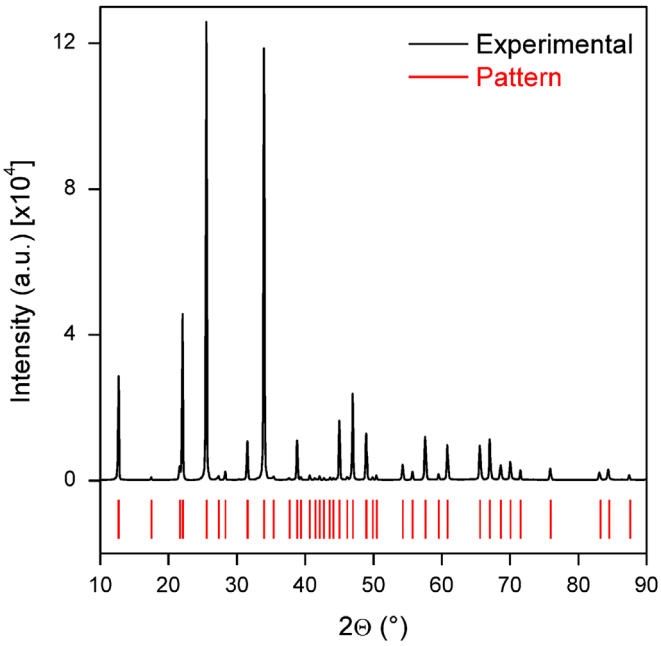

Fig. 1. X-ray diffraction of the willemite crystal.

Table 1
Main oxide components in (weight %) of willemite.

Sample	Compound (wt%)						
	SiO_2	ZnO	Al_2O_3	Fe_2O_3	MgO	CaO	MnO
Willemite	24.9	74.4	0.23	0.14	0.12	0.03	0.15

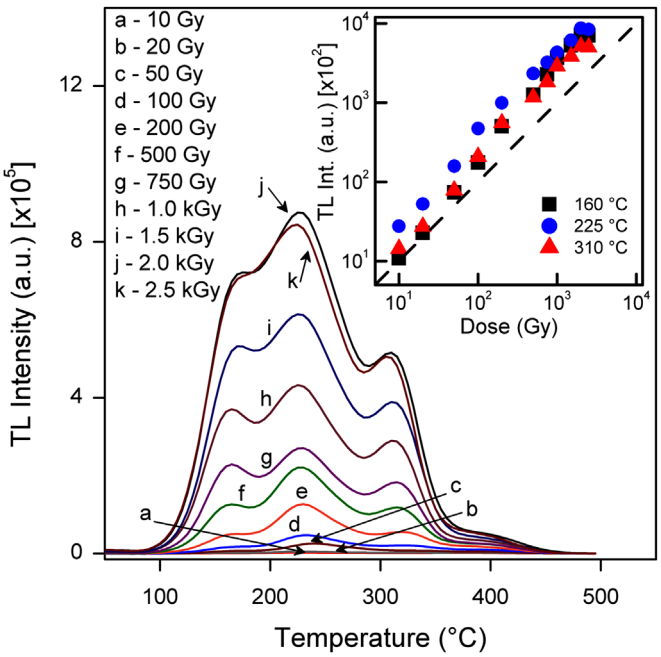

Fig. 2. TL glow curves of 500 °C thermally treated natural samples for 30 min and irradiated at several γ doses. In the inset of the figure, the TL intensity versus doses of the TL peaks at 160, 225 and 310 °C.

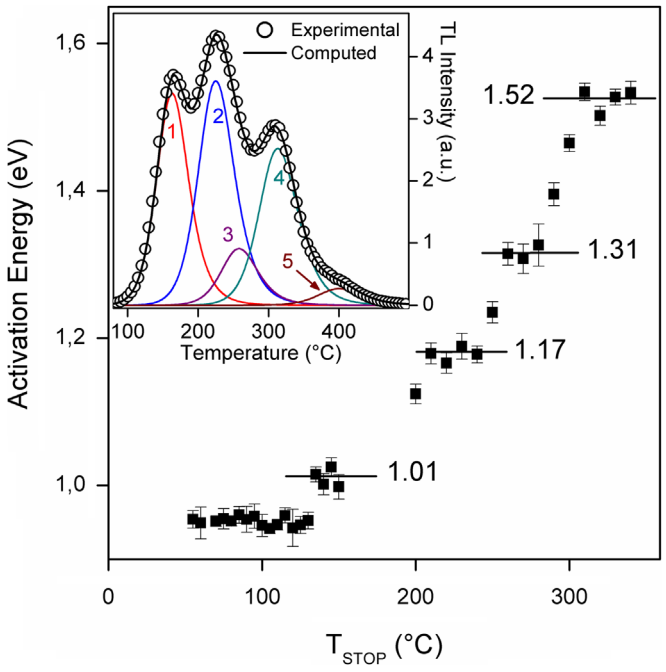

Fig. 3. Activation energy vs. T_{stop} obtained by the E–T_{stop} method. In inset, the TL glow curve from natural willemite pre-annealed at 500 °C and subsequently receiving a gamma-ray dose of 1 kGy. A good fit between the experimental glow curve (circles) and the simulated glow curve (full line) can be achieved by assuming the presence of five peaks.

Table 2
Activation energy (E), frequency factor (s) and lifetime (τ) of TL traps of willemite.

TL peak (°C)	E (eV)	s (s^{-1}) x10^{11}	τ (year at 25 °C)
160	1.01 ± 0.02	5.62 ± 1.23	0.007 ± 0.001
225	1.18 ± 0.01	2.30 ± 0.70	12 ± 1
260	1.32 ± 0.01	3.70 ± 0.80	1788 ± 195
310	1.52 ± 0.02	17.3 ± 3.3	$(9193 \pm 839)10^2$
400[a]	1.80	55.7	1545x10^7

[a] In the E–T_{stop} method the error could not be evaluated.

proposed by Kitis et al. [16] we obtain the deconvolution of the TL glow curve of willemite thermally pre-heated at 500 °C for 30 min and then gamma-irradiated with a dose of 1 kGy. The inset of Fig. 3 shows the five TL peaks separated using second order kinetics in the region between 50 and 500 °C. The deconvolution analysis has shown that the TL glow curve of the willemite crystal is composed of five peaks in the region between 50 and 450 °C. The positions, frequency factors (s), activation energies (E) and life times (t) of the TL peaks are presented in Table 2. The obtained high lifetime values of the 225, 260 and 310 °C TL peaks indicate its stability at room temperature and the linear behavior with gamma dose irradiation, allowing us to use the willemite crystal for dosimetric purposes.

The EPR spectrum at room temperature of gamma irradiated (dose: 10 kGy) willemite is shown in Fig. 4. On the basis of thermal annealing experiments, it is inferred that at least four defect centers contribute to the observed EPR spectrum. The EPR lines associated with these centers are labeled in Fig. 4. The EPR line labeled as center I in Fig. 4 is characterized by an isotropic g-value equal to 2.0114 and 4 G linewidth. Cation exchange disorder mentioned earlier and non-stoichiometry can lead to lattice defects in Zn_2SiO_4. First principal calculations suggest that the probability of formation of oxygen vacancies in a lattice with cation disorder is high as compared to a perfect cation-ordered system [17]. In this situation, F^+ centers will form with ease by trapping electrons at oxygen

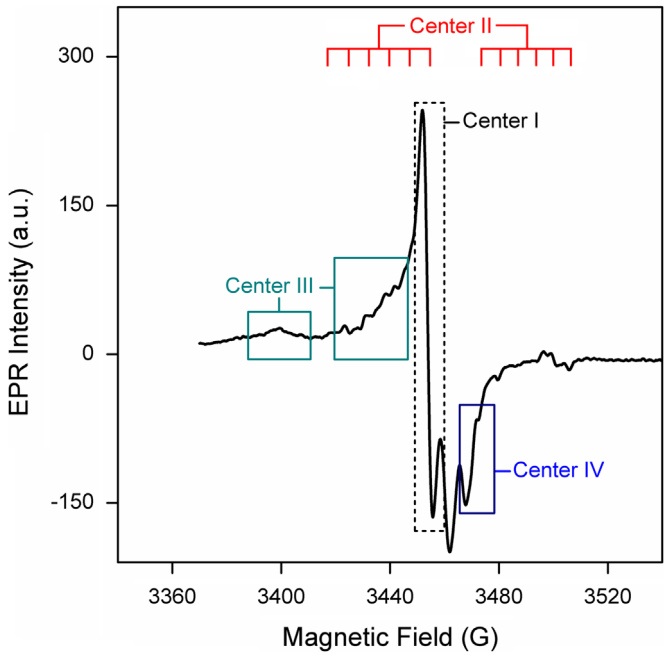

Fig. 4. Room temperature EPR spectrum of irradiated willemite (gamma dose: 10 kGy). Lines labeled as I and II are due to O^- ions. Center III line is assigned to an O_2^- ion and center IV characterized by an axial g-tensor is attributed to an F^+ center.

vacancies. On the other hand, cation vacancies can trap holes resulting in the formation of V-centers [18]. The slightly large g-shift of center I suggests that the center may be tentatively attributed to an O^- ion, which is formed by hole trapping at an oxygen ion, adjacent to a Zn-ion/Si-ion vacancy. O^- ion, in general is characterized by an axial g-tensor with the perpendicular component greater than g_e while the parallel component will nearly equals g_e. An example is the O^- ion in Magnesium Oxide [19]. On the other hand O^- ion also exhibits a rhombic g-tensor is some lattices. In a recent study on anatase nanoparticles, Misra et al. [20] observed the ion to have a rhombic g-tensor with principal values, $g_x=2.0$, $g_y=2.01$ and $g_z=2.03$. There have also been instances wherein an isotropic g-value is observed for the O^- ion.

The study on $MgAl_2O_4$ by Ibarra et al. [21] is one such case. $MgAl_2O_4$ after X-irradiation shows a center with similar features as center I. The g-value is 2.011 and an optical absorption band is observed at about 3.4 eV. On the basis of optical absorption spectra, the authors conclude that the center responsible for the EPR spectra and the associated absorption band is a hole trapped cation vacancy i.e., a V-type center formed by hole trapping at oxygen ions surrounding cation vacancies. In the present study on willemite, the assignment is mainly based on the findings of Ibarra et al. [21]. The EPR spectrum of center I is simulated and the simulated spectrum is given in Fig. 5. It is possible that there may be a parallel component EPR line for center I but difficult to see due to overlap of lines from other centers. A pulsed-thermal annealing method was used to measure the stability of center I. After heating the sample up to a given temperature, where it is maintained for 3 min, it is cooled rapidly down to room temperature for EPR measurements. Fig. 6 shows the thermal annealing behavior of center I. It is observed that the center becomes unstable around 110 °C and decays in the temperature range 110–210 °C. This decay appears to relate to the TL peak at 160 °C.

Apart from the EPR line of center I seen near free-electron resonance, a multiple line spectrum of low intensity is observed in this region with lines extending over a magnetic field range of about 100 G (Fig. 4). These low intensity lines seem to originate

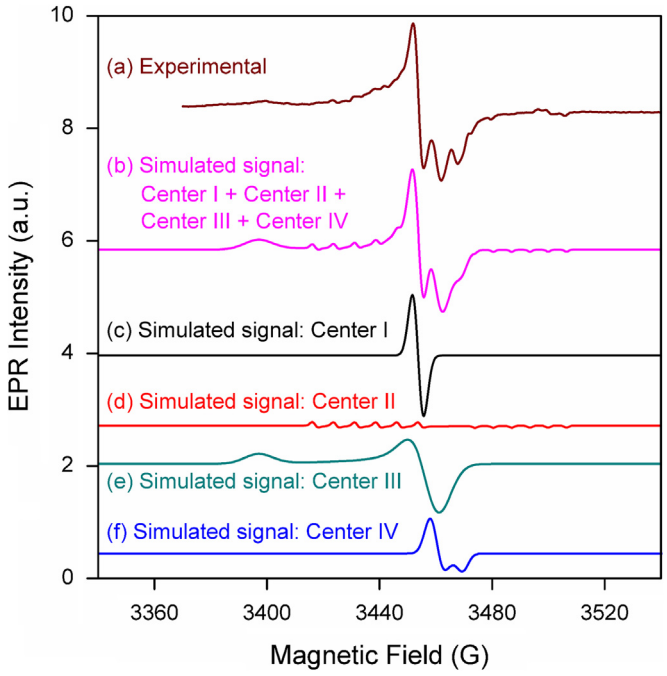

Fig. 5. EPR spectra of willemite (a) experimental, (b) simulated signal Center I+Center II+Center III+Center IV, (c) simulated signal Center I, (d) simulated signal Center II, (e) simulated signal Center III and (f) simulated signal Center IV.

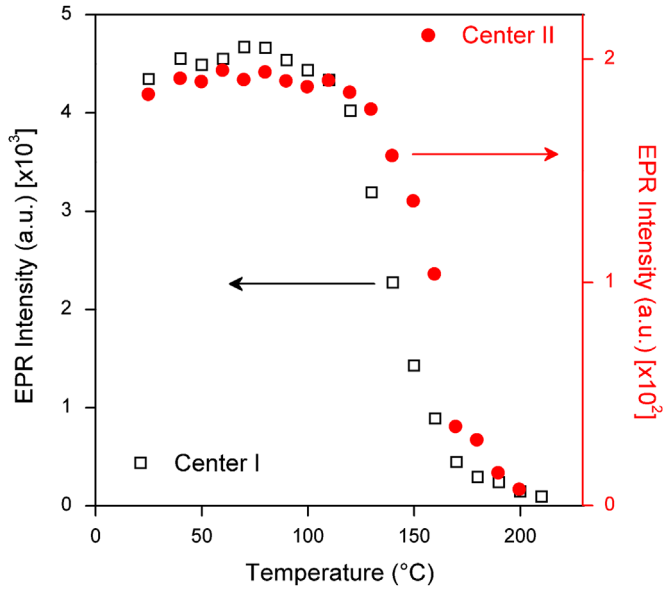

Fig. 6. Thermal annealing behavior of center I (□ black square) and center II (● red circle) in willemite.

from the hyperfine interaction of the unpaired electron with nearby nuclei. In willemite (Zn_2SiO_4), zinc (^{67}Zn, 4.1% abundance) as well as silicon (^{29}Si, 4.7% abundance) have isotopes with nuclear spin. Further, chemical analysis has indicated the presence of aluminum as an impurity in the willemite mineral and aluminum ^{27}Al (nuclear spin 5/2 and magnetic moment: 3.142) has an abundance of 100% [22].

It was mentioned earlier that cation disorder and non-stoichiometry of Zn_2SiO_4 can give rise to O^- ions, which are formed by hole trapping at zinc or silicon vacancies. Hence, center II is tentatively assigned to an O^- ion (2) stabilized by a nearby cation vacancy (a hole trapped in a Zn^{2+}/Si^{4+} ion vacancy). It has been observed that O^- type hole centers in some cases exhibit hyperfine interaction due to adjacent ions. For example, in an earlier study on $LiNbO_3$ [23], it has been observed that the O^- hole center exhibits hyperfine structure due to three neighboring ions. On the other hand, in Li_3VO_4, Murata et al. [24] have observed that the O^- ions interacts with one vanadium ion. In Li_3VO_4, each oxygen has one nearest neighbor vanadium ion and consequently, the O^- ion formed in this system shows hyperfine interaction with the nearest neighbor vanadium ion. In a similar way, the hole trapped by oxygen in willemite [O^- ion (2)] could be interacting with nearest cations giving rise to the observed spectrum. On the basis of the observed multiple line spectrum it is speculated that the possibility of the unpaired electron interacting with aluminum (^{27}Al) is more due to the ion´s larger abundance. The higher spread of the spectrum is perhaps consistent with the ^{27}Al ion's higher magnetic moment and higher nuclear spin. Assuming an axial g-tensor for center II with principal values $g_{\parallel}=1.9974$ and $g_{\perp}=2.029$ and also assuming an interaction of the unpaired electron with ^{27}Al nucleus ($A_{\parallel}=6.5$ G and $A_{\perp}=7.5$ G), the EPR spectrum of center II has been simulated and the simulated spectrum is shown in Fig. 5. Fig. 5 shows also the simulated spectrum arising from the contribution of centers I, II, III and IV and it is seen that there is reasonable agreement between the experimental and simulated spectra. It is observed that the principal g-values of center II as derived from the simulation are in accordance with the expectations of an O^- ion [19]. The thermal annealing behavior of center II is shown in Fig. 6. It is observed that the center becomes unstable around 120 °C and decays in the temperature range 120–200 °C. Hence, O^- ion (center II) could also be associated with the 160 °C TL peak along with O^- ion (center I).

Center III shown in Fig. 4 does not exhibit any hyperfine structure and is characterized by an axially symmetric g-tensor with principal values $g_{\parallel}=2.0451$ and $g_{\perp}=2.011$. Center III lines are seen more clearly after thermal anneal at 250 °C and this spectrum is shown in Fig. 7. A simulated spectrum of center III using the g-values $g_{\parallel}=2.0507$ and $g_{\perp}=2.0145$ is shown in Fig. 5. In general, the most likely centers to be formed on gamma irradiation in a system like willemite are the V-centers, F-centers and F^+-centers (an electron trapped at an anion vacancy). In a study on the binary oxide system Y_2O_3–CaO, Osada et al. [25] have observed oxygen ions. EPR studies have shown that the ion is characterized by an axial g-tensor with principal values $g_{\parallel}=$ 2.040 and $g_{\perp}=2.0030$. The oxygen ion has been ascribed to the superoxide ion O_2^- and is generated by adsorption of molecular oxygen by the binary oxide system. O_2^- ions with considerable g-anisotropy have also been observed in a number of zeolites and metal oxides [26–28]. It is to be noted that the $g_{\parallel}$ value for the O_2^- ion was found to be highly matrix dependent and ranged between 2.015 and 2.080. Based on these results, center III with a relatively large anisotropy in g-values in the present system is tentatively assigned to an O_2^- ion. The thermal annealing behavior of center III is shown in inset of the Fig. 7. It is observed that the center becomes unstable around 120 °C and decays in the broad temperature range 120–370 °C. This decay appears to relate to the TL peak at 160 °C and also may contribute to the dominant TL peaks at 225 and 260 °C.

The EPR line labeled as IV in Fig. 4 is due to a center characterized by an axially symmetric g-tensor with principal values $g_{\parallel}=2.0025$ and $g_{\perp}=2.0088$. The axial nature of the spectrum could be seen more clearly in thermal annealing experiments and Fig. 8 shows this spectrum which is recorded after thermal anneal at 400 °C.

A probable center which can be trapped in the present system is the F^+ center (an electron trapped at an anion vacancy). In an alkali halide system like LiF, the F center (an electron trapped at the F^- ion vacancy) displays a large linewidth of about 100 G [29]. The center has a g-value close to the free-spin value. However, the inherent linewidth of F^+ center is about 1 G and is observed in MgO system [30]. The linewidth is determined by the delocalization of

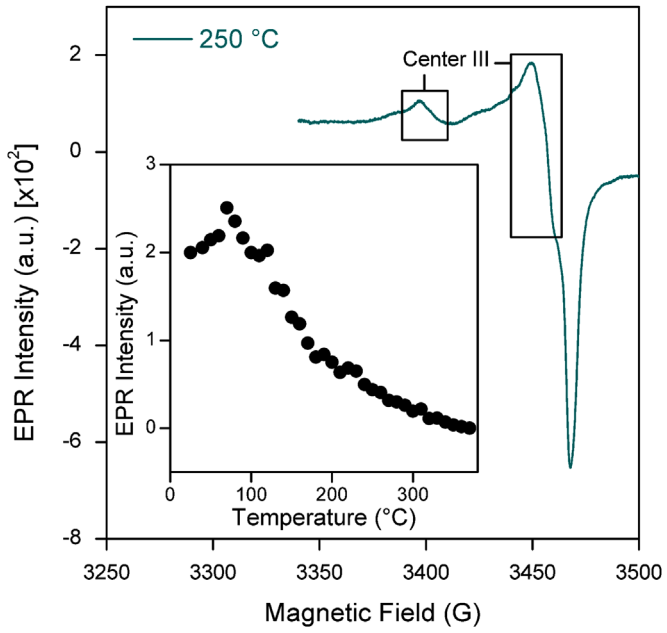

Fig. 7. Room temperature EPR spectrum of irradiated willemite after thermal anneal at 250 °C showing EPR lines due to center III. Inset shows the thermal annealing behavior of center III in willemite.

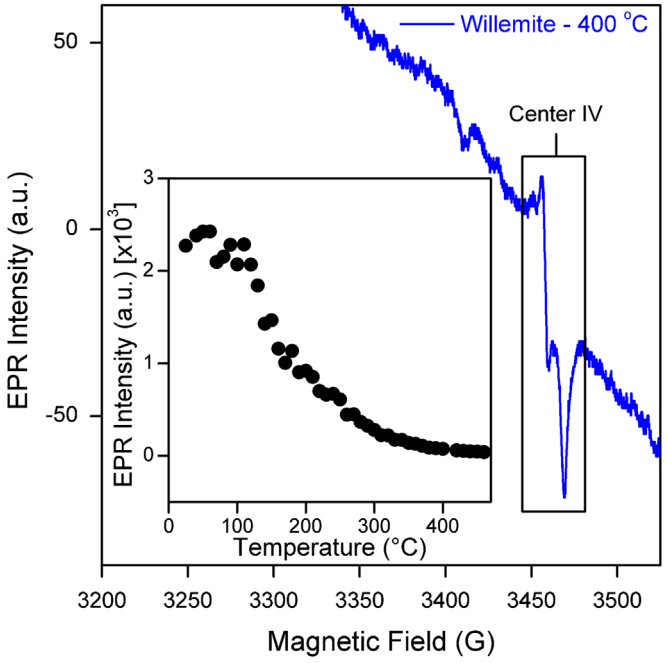

Fig. 8. Room temperature EPR spectrum of irradiated willemite after thermal anneal at 400 °C displaying EPR lines due to center IV. Inset shows the thermal annealing behavior of center IV in willemite.

the unpaired electron and also on the ions present in a system. In systems like alkali halides, there is considerable delocalization and the electron interacts with several alkali and halide ions from successive neighboring shells.

Centers with an electron trapped at an anion vacancy (i.e., F^+ centers) have also been observed in oxide systems. The basic features of these centers are the *g*-values which are close the free-electron value with a *g*-shift which may be positive or negative. A recent observation of this center is in pure and defective TiO_2 nanoparticles [31]. Defect center IV formed in the present system is characterized by a relatively small *g*-shift and the linewidth is not large. On the basis of these observations and considerations of the characteristic features of the defect centers likely to be formed in a system such as willemite (Zn_2SiO_4), center IV is tentatively assigned to an F^+ center.

In general, F^+ centers are characterized by an isotropic *g* value and in the present study, center IV exhibits an axially symmetric *g*-tensor. Systems like $CaZrO_3$:Tb [32] as well as yttria stabilized zirconia (YSZ), i.e. ZrO_2:Y [33] exhibit a center which shows an axially symmetric *g*-values. In YSZ, the principal *g*-values are $g_{\|}=1.996$ and $g_{\perp}=1.972$ and the *g*-values are seen to be smaller than the free-electron value. These centers were identified as F^+-centers. The axial nature of the *g*-values in YSZ were interpreted by considering the presence of a symmetry breaking defect at an anionic site near the F^+-center. The symmetry breaking defect was considered to be the neutral F-center (oxygen vacancy with two electrons) which has a high probability of forming in YSZ lattice owing to the presence of a large density of oxygen vacancies present in this system. Center IV in the present system is also identified as an F^+-center and the center needs to be in the vicinity of an F-center which results in the observed features. Oxygen vacancies may be present in Zn_2SiO_4 lattice due to reasons mentioned earlier. Irradiation can then lead to the formation of F-center in close proximity to center IV. It may be mentioned that an F^+-center in X-irradiated sodium β-alumina also exhibits an axial *g*-tensor with positive *g*-shifts [34] as in the present case.

The thermal annealing behavior of center IV is shown in inset of Fig. 8. The intensity of the EPR line associated with this center appears to decrease in two stages. The initial decay is in the range 100–240 °C and this may be associated with the TL peaks at 160 and 225 °C. On the other hand, the second stage is in the temperature region 240–420 °C and this correlates with the TL peaks at 260 and 310 °C. It is speculated that the charges released from defect centers are combining with center IV rendering this center as a possible recombination center for the 160 and 225 °C TL peaks and perhaps also for the peaks at 260 and 310 °C.

4. Conclusions

Willemite mineral exhibits TL glow peaks at about 160, 225, 260, 310 and 400 °C. Four defect centers have been identified in the irradiated mineral. These centers are tentatively assigned to O^- ions, O_2^- ion and F^+ center. O^- ion (1) correlates with the 160 °C TL peak while O^- ion (2) is also associated with this TL peak. A broad decay is exhibited by the O_2^- ion which relates to the TL peak at 160 °C and also may contribute to the main dominant peaks at 225 and 260 °C. The F^+ center appears to act as a recombination center for the 160 and 225 °C TL peaks as well as for the peaks at 260 and 310 °C.

Acknowledgments

The authors wish to thank Ms. E. Somessari and Mr. C. Gaia, Instituto de Pesquisas Energeticas e Nucleares (IPEN), Brazil, for kindly carrying out the irradiation of the samples. To FAPESP (Process number 2014/03085-0) for partial financial support and to CAPES (Process number BEX-9612130) for fellowship to T.K. Gundu Rao.

References

[1] C. Hang, M.A. Simonov, N.V. Belov, Phys. Crystallogr. 15 (1970) 387.
[2] M.M. Kuklja, J. Phys.: Condens. Matter 12 (2000) 2953.

[3] A.P. Patel, M.R. Levy, R.W. Grimes, R.M. Gaume, R.S. Frigelson, K.J. McClellan, C. R. Stanek, Appl. Phys. Lett. 93 (2008) 191902.
[4] J. Dong, K. Lu, Phys. Rev. B 43 (1991) 8808.
[5] Q.D. Truong, M.K. Devaraju, T. Tomai, I. Honma, ACS Appl. Mater. Interfaces 5 (2013) 9926.
[6] N. Basavaraju, K.R. Priolkar, D. Gourier, S.K. Sharma, A. Bessiere, B. Viana, Phys. Chem. Chem. Phys. 17 (2015) 1790.
[7] H.X. Zhang, S. Buddhudu, C.H. Kam, Y. Zhou, Y.L. Lam, K.S. Wong, B.S. Ooi, S. L. Ng, W.X. Que, Mater. Chem. Phys. 68 (2001) 31.
[8] J. Lin, D.U. Sänger, M. Mennig, K. Bärner, Thin Solid Films 360 (2000) 39.
[9] Q.Y. Zhang, K. Pita, W. Ye, W.X. Que, Chem. Phys. Lett. 351 (2002) 163.
[10] Q.Y. Zhang, K. Pita, C.H. Kam, J. Phys. Chem. Solids 64 (2003) 333.
[11] N.F. Cano, A.R. Blak, S. Watanabe, Phys. Chem. Miner. 37 (2010) 57.
[12] N.F. Cano, L.H. Santos, J.F.D. Chubaci, S. Watanabe, Spectrochim. Acta A 137 (2015) 471.
[13] N.F. Cano, A.R. Blak, J.S.A. Arenas, S. Watanabe, J. Lumin. 131 (2011) 165.
[14] S.W.S. McKeever, Phys. Status Solidi (a) 62 (1980) 331.
[15] S.W.S. McKeever, Thermoluminescence of Solids, Cambridge University Press, Cambridge, 1985.
[16] G. Kitis, J.M. Gomez-Ros, J.W.N. Tuyn, J. Phys. D: Appl. Phys. 31 (1998) 2636.
[17] N. Yuan, X. Liu, F. Meng, D. Zhou, J. Meng, Ionics 21 (2015) 1675.
[18] M.S. Holston, J.W. McClory, N.C. Giles, L.E. Halliburton, J. Lumin. 160 (2015) 43.
[19] W.B. Williamson, J.H. Lunsford, Chem. Phys. Lett. 9 (1971) 33.
[20] S.K. Misra, S.I. Andronenko, D. Tipikin, J.H. Freed, V. Somani, O. Prakash, J. Magn. Magn. Mater. 401 (2016) 495.
[21] A. Ibarra, F.J. López, M. Jiménez de Castro, Phys. Rev. B 44 (1991) 7256.
[22] R.C. Weast (Ed.), Handbook of Chemistry and Physics, CRC, Cleveland, 1971.
[23] T. Miki, M.R. Hantehzadeh, L.E. Halliburton, J. Phys. Chem. Solids 50 (1989) 1003.
[24] T. Murata, T. Miki, J. Appl. Phys. 73 (1993) 1110.
[25] Y. Osada, S. Koike, T. Fukushima, S. Ogasawara, T. Shikada, T. Ikariya, Appl. Catal. 59 (1990) 59.
[26] D.D. Eley, M.A. Zammitt, J. Catal. 21 (1971) 366.
[27] K.M. Wong, J.H. Lunsford, Phys. Chem. 74 (1971) 1165.
[28] J.H. Lunsford, Catal. Rev. 8 (1974) 135.
[29] C.A. Hutchison, Phys. Rev. 75 (1949) 1769.
[30] J.E. Wertz, P. Auzins, R.A. Weeks, R.H. Silsbee, Phys. Rev. 107 (1957) 1535.
[31] B. Choudhury, A. Choudhury, Sci. Adv. Mater. 6 (2014) 2115.
[32] S. Vijay Singh, Watanabe, T.K. Gundu Rao, Katharina Al-Shamery, M. Haase, Y. D. Jho, J. Lumin. 132 (2012) 2036–2042.
[33] J.M. Costantini, F. Beuneu, D. Gourier, C. Trautmann, G. Calas, M. Toulemonde, J. Phys.: Condens. Matter 16 (2004) 3957.
[34] K. O'Donnell, R.C. Barklie, B. Henderson, J. Phys. C: Solid State Phys. 11 (1978) 3871.